MASSACHUSETTS INSTITUTE OF TECHNOLOGY

ARTIFICIAL INTELLIGENCE LABORATORY

A. I. Memo No. 465

February 1978

LANDSAT MSS Coordinate Transformations

by

Berthold K. P. Horn

Robert J. Woodham

ABSTRACT. A number of image analysis tasks require the registration of a surface model with an image. In the case of satellite images, the surface model may be a map or digital terrain model in the form of surface elevations on a grid of points. We develop here an affine transformation between coordinates of Multi-Spectral Scanner (MSS) images produced by the LANDSAT satellites, and coordinates of a system lying in a plane tangent to the earth's surface near the sub-satellite (Nadir) point.

This report describes research done at the Artificial Intelligence Laboratory of the Massachusetts Institute of Technology. Support for the laboratory's artificial intelligence research is provided in part by the Advanced Research Projects Agency of the Department of Defense under Office of Naval Research contract number N00014-75-C-0643.

1. Introduction.

Some image analysis tasks depend on the availability of a registered surface model. Registration can be accomplished using manually identified ground control points or by matching the real image with a synthetic image calculated from the surface model using assumed reflectance properties. In either case, the form of the transformation from image coordinates to model coordinates must be known. The registration process is then used to determine the unknown parameters of the transformation.

We show here that in the case of satellite images obtained by a mechanical scanning system, such as that used on the LANDSAT satellites, an affine transform applies, if small, second-order effects are neglected. Such a transformation has six parameters which depend on the state of the scanning platform. Each parameter is exhibited as a function of the components of this state and other relevant fixed quantities. These equations can then be used to predict transformation parameters if the state of the scanning platform is known.

A possible application of automatic registration of images and surface models is the determination of the parameters of a satellite's orbit. Unfortunately, a rigid body has six degrees of freedom (position and attitude) and so its state has twelve components (position, velocity, attitude and attitude rate). Clearly, then, knowing the six parameters of the affine transformation at one instant of time is not sufficient to permit a calculation of the vehicle's state.

A series of determinations of the transformation for images taken of different areas of the earth, however, may permit determination of the vehicle's orbit. If we ignore small perturbations, then the position and velocity of

the center of mass of the vehicle at one instant of time fully determine its orbit. We prefer to use orbital parameters to describe this component of the state in some circumstances.

2. Basic Orbital Geometry.

LANDSAT is in a near-polar, retrograde, sun-synchronous orbit which is nearly circular. The nominal parameters of this orbit include a semi-major axis of 7,294,690 meters, that is, 916,525 meters above an earth with equational radius of 6,378,165 meters and oblateness of 1 in 298.3. The nominal period is 103.267 minutes, which brings the sub-satellite point back to the same spot on earth after 251 orbits in 18 days. At the equator, neighboring sub-satellite tracks are spaced 159,380 meters. The descending node is nominally passed at 9:42 A.M. The orbital inclination is nominally 99.092°, which brings the satellite within $\varepsilon \approx 9.092°$ of the north pole at the vertex V (see Figure 1). All of the parameters drift with time due to perturbing influences such as solar wind, light pressure, atmospheric drag, non-spherical distribution of masses in the earth, effects of mass expulsion, and so on. The orbit is re-adjusted at time using small gas discharges to maintain the positions of the ground-tracks within about 35 km of nominal and to prevent the time of north to south crossing of the equator from drifting too far from the nominal 9:42 A.M. The orbital data is derived from radio tracking information.

Points on the orbit may be conveniently referenced to the vertex V. The orbital travel distance ρ is measured from it, and the reference meridian passes through it. The change in geographical longitude λ_s is measured from the reference meridian (see Figure 1).

Ignoring for a moment the rotation of the earth, we find that the nominal position of the satellite, S_s, lies at (geocentric) latitude ϕ'. The nominal heading of the satellite relative to the local meridian is given by the angle H_s. The relationship between orbital parameters ε, ρ and the geographical co-

ordinates λ_s, ϕ' can be established using products of rotation matrices [1]. Here we follow a more direct route using spherical trigonometry.

Considering the right spherical triangle N E_s S_s (see Figure 1), applying the sine theorem, one finds that

$$\sin(\phi')/\sin(90° - \varepsilon) = \sin(90° - \rho)/\sin(90°)$$

or,

$$\sin \phi' = \cos \varepsilon \cos \rho \tag{1}$$

Next, from right spherical triangle V P S_s, one finds,

$$\sin \lambda_s/\sin \rho = \sin H_s/\sin \varepsilon$$

and, applying the cosine theorem (for angles),

$$\cos \lambda_s = - \cos H_s \cos 90° + \sin H_s \sin 90° \cos \rho$$

or,

$$\cos \lambda_s = \sin H_s \cos \rho$$

Hence,

$$\tan \lambda_s = \tan \rho/\sin \varepsilon \tag{2}$$

Equations (1) and (2) determine geographical coordinates ϕ', λ_s in terms of orbital parameters ε, ρ. Similarly,

$$\cos H_s = - \cos \lambda_s \cos 90° + \sin \lambda_s \sin 90° \cos \varepsilon$$

or,

$$\cos H_s = \sin \lambda_s \cos \varepsilon$$

Hence,

$$\tan H_s = \tan \varepsilon / \sin \rho \qquad (3)$$

Equation (3) determines nominal heading H_s in terms of orbital parameters ε, ρ.

As it turns out, the earth does rotate and so the sub-satellite point is displaced an additional amount in the direction of the local geographical parallel, from point S_s to point S. The latitude ϕ' remains unchanged, of course, while the longitude is increased by λ_e and the sub-satellite track deviates by an angle H_e from the nominal direction. In order to calculate these quantities, one must know the angular velocities of the earth and of the satellite in its orbit. Let these quantities be ω_e and ω_s, respectively.

Since the satellite retraces its path almost exactly every 18 days, after completing 251 orbits, we know the ratio of these two quantities,

$$r_\omega = \omega_e / \omega_s = d \lambda_e / d\rho = 18/251 \qquad (4)$$

Then,

$$\lambda_e = r_\omega \rho \tag{5}$$

Actually, ω_s is not constant, unless the satellite is in a circular orbit -- we will return to this point later.

At latitude ϕ', the earth surface is displaced a distance $R\omega_e \cos \phi' \, dt$ in a time interval dt, where R is the distance of the surface from the earth's center.

The calculation of the change in heading is a little bit more complicated. If we let the satellite heading $H = H_e + H_s$, then one can see that (Figure 2)

$$\tan H = (r_\omega \cos \phi' + \sin H_s)/\cos H_s \tag{6}$$

Next,

$$\tan H_e = \tan (H - H_s) = (\tan H - \tan H_s)/(1 + \tan H \tan H_s)$$

$$\tan H_e = r_\omega \cos \phi' \cos H_s/(1 + r_\omega \cos \phi' \sin H_s) \tag{7}$$

Now, from the right spherical triangle P V S_s (Figure 1), one obtains

$$\sin (90° - \phi')/\sin (90°0) = \sin \rho/\sin H_s$$

That is,

$$\cos \phi' \sin H_s = \sin \varepsilon \tag{8}$$

Similarly, one finds,

$$\sin (90° - \phi')/\sin (90°) = \sin \rho/\sin \lambda_s$$

That is,

$$\cos \phi' = \sin \rho/\sin \lambda_s \tag{9}$$

In deriving (3), we determined that $\cos H_s = \sin \lambda_s \cos \varepsilon$, so that

$$\cos \phi' \cos H_s = \sin \rho \cos \varepsilon \tag{10}$$

Finally, we can use equations (8) and (10) to simplify the expression for H_e (7),

$$\tan H_e = r_\omega \cos \varepsilon \sin \rho/(1 + r_\omega \sin \varepsilon) \tag{11}$$

Equation (11) determines H_e in terms of orbital parameters ε, ρ and the constant r_ω. Note that $r_\omega \sin \varepsilon$ is quite small (.0112) and can be ignored in approximate calculations [1].

Also, now using (8) and (10), we can simplify the expression for tan H (6),

$$\tan H = (r_\omega \cos^2 \phi' + \sin \varepsilon)/(\cos \varepsilon \sin \rho)$$

or,

$$\tan H = [r_\omega(1 - \cos^2 \varepsilon \cos^2 \rho) + \sin \varepsilon]/[\cos \varepsilon \sin \rho] \tag{12}$$

To sum up, given ε and ϕ', we find the orbital travel distance ρ using equation (1), the longitude relative to the reference meridian $\lambda = \lambda_s + \lambda_e$ using equations (2) and (5) and the heading $H = H_s + H_e$ using equations (3) and (11), or (12).

3. Local Solar Time at the Point of Observation.

An immediate application of the results developed so far is the determination of the local solar time at the sub-satellite point. (This gives one some idea of what the position of the sun is likely to be). Let the time of the descending node be T_o. That is, the satellite crosses the equator from North to South when the local solar time is T_o (for LANDSAT this is nominally 9:42 A.M., but tends to vary as the orbit drifts and is readjusted).

If a point is observed when the satellite has progressed ρ in its orbit from the vertex V, then it still has to travel through an angle $(90° - \rho)$ before reaching the equator. This will take an amount of time which can be expressed in hours as $r_\omega(90° - \rho)/15$.

Furthermore, the point of observation lies $(90° - \lambda_s)$ ahead of the point of equator crossing in longitude. Thus the local solar time is later by a time which, when expressed in hours, comes to $(90° - \lambda_s)/15$. Finally, then, one sees that the local solar time at the sub-satellite point is

$$T = T_o + (90° - \lambda_s)/15 - r_\omega(90° - \rho)/15 \qquad (13)$$

where $\tan \lambda_s = \tan \rho / \sin \varepsilon$ (2). Because $r_\omega = 18/251$, one finds that the first term predominates. As a result, points North of the equator, imaged <u>earlier in the orbit</u>, are observed at local solar time <u>after</u> T_o, while points South of the equator, imaged later in the orbits, are observed at local solar time before T_o.

4. The Scanning Platform.

The satellite uses an oscillating mirror to produce the across-the-track scan. Individual lines of the image are obtained by this means. The satellite's motion in orbit provides for the other scanning direction. Successive lines are displaced along the sub-satellite track. Nominally, the optical system points straight down and the mirror scanning motion is perpendicular to the velocity vector of the vehicle. In practice, there are small but significant departures from this ideal state (Figure 3).

Pitch and roll are measured to an accuracy of .07° using horizon scanners sensitive to the infrared radiation (around 14 μm) emitted by the atmosphere. Yaw is measured with similar accuracy using a gyro compass. Pitch and roll are maintained within ± .4° using the vehicle's attitude control system, while yaw is maintained within ± .7°. A major component of the attitude control system is a set of inertia wheels which are used in order to keep down gas expenditure.

An attempt is also made to minimize rates of change of attitude which result from adjustments. The maximum attitude rates are .015 degree/second. Attitude rates are estimated from time-histories of measured attitudes. For further information on the scanning platform and its motion, see references [1 - 4].

Ground tracking information provides good ephemeris data. However, since a picture cell in the image is only about 79 meters by 56 meters, one cannot expect the position of the satellite to be known accurately enough to predict exactly which point of the earth is imaged. Similarly, on-board horizon sensors permit a good determination to be made of the attitude of the satellite

platform. Nevertheless, these measurements are not accurate enough to permit the direct calculation of the ground coordinates corresponding to a particular picture cell. Errors of several kilometers may be encountered when this is attempted [3].

"Precision processing" of satellite image information entails the manual identification of known ground control points on each image and the derivation of a suitable transformation based on this information. So far, this has proved too expensive and LANDSAT images are "bulk processed", that is, treated as if the calculated position and attitude of the satellite were exact. As a result, the final photographic products may have errors in translation of several kilometers. Fortunately, non-linear effects introduced by this approximation are small.

One might envision systems which automatically register image information with map or surface model information. In such a system, one has to model the imaging operation so that the registration process can be used to determine the unknown parameters, such as satellite position and attitude. A clear understanding of the scanning process is required to accomplish this.

5. Fineness of the Scanner Model.

A large variety of effects contribute to the imaging transformation. Amongst these are large effects which must be considered, such as the motion of the satellite in its orbit and the rotation of the earth beneath it. There are also smaller effects which have to be judged individually. Some of these produce non-linear effects. Examples are panoramic scan distortion (the mirror scans evenly in angle, not tangent of the angle), perspective projection (which can be dealt with only if a surface model is available) and second-order effects of errors in attitude of the spacecraft. The relative importance of these effects has already been discussed by others [1 - 4]. The most important criterion for including an effect in our model was linearity.

Fortunately, all major components of the image transformation turned out to produce linear transformation of image coordinates. Second order, non-linear effects were neglected, but turn out to contribute errors which are typically smaller than a picture cell in size. Compounding these linear transformations leads to an overall affine transformation which is easy with which to deal. Such a transformation has six parameters, which may be found using the registration of the image with some surface information in the form of a map or a digital terrain model.

The six parameters, as one might expect, depend rather directly on the position of the satellite in its orbit, the attitude of the scanning platform, the orbital velocity, and the mirror-sweep velocity. It is conceivable that a system which automatically determined the parameters of the affine transformation using a matching process of real with synthetic images obtained form a terrain model, could also then proceed to estimate the underlying orbital data. A

satellite equipped with such a system would be able to determine its position or attitude more accurately than it might using predicted ephemeris data obtained from expensive ground tracking efforts.

6. Nominal Parameters of LANDSAT Imaging System (Orbital Parameters Drift).

Orbit:

Apogee ≈ 917 km Perigee ≈ 898 km
Inclination ≈ 99.1° (Retrograde orbit)
Anomalistic period ≈ 103.267 minutes
[That is, 251 orbits in 18 days]
Equatorial Earth radius ≈ 6378 km
Polar Earth radius ≈ 6357 km
Equatorial speed of rotation ≈ 463.8 m/sec
Average ground track speed of satellite ≈ 6457 m/sec

Mirror-Scanner:

Frequency = 13.260 Hertz
[That is, 6 lines are scanned every 73.42 msec]
One line every 12.237 msec
Lines spaced by ≈ 79.0 meters at nominal height
390 scans per image
That is, 2340 scan-lines per image
[This takes 28.63 seconds and covers ≈ 185 km]

Pixel Information:

Instantaneous field of view ≈ 79 m x 79 m
Mirror amplitude ≈ ±2.886°
Total scan distance ≈ 11.545°
That is ≈ 185 km at nominal altitude
Pixels per line (nominal) ≈ 3240
Sampling interval = 9.958 μsec
That is, about 55.8 - 56.5 m on the ground
Consequently, $\omega_m \simeq 6.21$ radians/second
Time to scan (six) lines (in parallel) ≈ 32.238 msec

Total Image Size: ≈ 2340 x 3240 ≈ 7,581,600 pixels

7. Image Coordinate Transformation.

Let the pixels be numbered sequentially within each scan line and let the scan lines be numbered sequentially. Then x_s will be the number of a pixel counted from the beginning of a scan-line, while y_s will be the number of a line counted from the beginning of a particular image. (Actually, this is arbitrary since the scanner does not start or stop at image boundaries; the continuous stream is segmented into images by ground processing). These will be called satellite coordinates.

Now erect a coordinate system in the region of interest. First construct a tangent plane and let the x-axis run in the west-to-east direction, and the y-axis in the south-to-north direction. Now add a z-axis going vertically up (we ignore the non-spherical nature of the earth and other such minor effects). We will use the notation (x_e,y_e) for points on the surface. The satellite can also be located in this earth coordinate system. At some reference time t_o, it is at (x_o,y_o,z_o) and has attitude α(roll), β(pitch), and γ(yaw) (Figure 3). The three attitude angles will be assumed to be small.

At time t_o, the scanner will also be at a particular point in its scan of the image. Let it be scanning the x_{so}-th pixel in the y_{so}-th line of the image. If the sensor were pointing straight down (that is, $\alpha = 0$ and $\beta = 0$), it would be imaging the sub-satellite point (x_o,y_o) (Figure 4).

At this point we introduce a convenient artifice, a spherical earth fixed relative to the orbit of the satellite. That is, a spherical surface which is also sun-synchronous, rotating once a year. Later we will take into account the fact that the earth rotates underneath the satellite. We will first develop the coordinate transformation for the case of a fixed surface because

it is easier to understand this transformation.

Here it is convenient to refer pixel locations to the reference point (x_{so}, y_{so}) (Figures 4 and 5).

$$x_1 = (x_s - x_{so}) \qquad \text{and} \qquad y_1 = (y_{so} - y_s) \tag{14}$$

Let the angular scanning velocity produced by the mirror during its linear phase be ω_m (about 6.21 rad/sec) and let t_s (9.958 μsec) be the sampling interval during the scan, then, on a surface at a distance z_o from the satellite and perpendicular to the extension of the optical axis of its scanning system, we find a cross-track scanning amplitude x_2 as follows,

$$x_2 = (\omega_m \, z_o \, t_s) \, x_1 \tag{15}$$

In the along-the-track direction, the motion of the satellite in its orbit provides for the scanning and so,

$$y_2 = (\omega_s \, R \, t_\ell) \, y_1 \tag{16}$$

where R is the distance of the surface from the center of the earth (about 6370 km), while ω_s is the angular velocity of the satellite in its orbit (about 1.014 milli-rad/sec) and t_ℓ is the interval between successive scan-lines (12.237 milli-seconds). [Actually <u>six</u> lines are scanned simultaneously every 73.42 milli-seconds.]

At this point, we note that because of possibly non-zero yaw, the across-

track scanning may not be perfectly perpendicular to the along-track scan. This skewing effect can be taken care of as follows (Figure 6),

$$x_3 = x_2 \cos \gamma \qquad \text{and} \qquad y_3 = y_2 - x_2 \sin \gamma \tag{17}$$

We still have to deal with the effects of roll and pitch. For small angles, these will have the effect of shifting the imaged area by an amount proportional to the product of the angles and the distance to the surface being imaged. Secondary, non-linear effects (such as bending of the scanning line) will be ignored, as will non-commutativity of rotations.

Thus the effects of non-zero roll and pitch can be introduced,

$$x_4 = x_3 - \alpha z_0 \qquad \text{and} \qquad y_4 = y_3 - \beta z_0$$

where z_0 is the height of the satellite above the surface as before. The co-ordinate system above lies on the tangent place of the (fixed) sphere. One coordinate axis (y) points backward along the sub-orbital track, while the other (x) lies at right angles to it. We would prefer to work with a system which is aligned with local north. The angle between the local meridian and the sub-satellite track (on the fixed earth) is H_s. We can rotate coordinates into a new system as follows (Figure 7),

$$x_5 = x_4 \cos H_s + y_4 \sin H_s \tag{19}$$

$$y_5 = -x_4 \sin H_s + y_4 \cos H_s \tag{20}$$

In this new coordinate system, the y-axis points north and the x-axis east. Finally, we are ready to introduce the rotation of the earth. It has no effect on the value of y, of course, but does introduce a shift in x which depends on the time when a particular pixel is imaged. For a particular line of the image, this time can be calculated relative to the time t_o, when the reference line was imaged. For line number y_s, this time interval equals $t_\ell(y_s - y_{so}) = -t_\ell y_1$. In this time interval, the earth has rotated in an easterly direction by an amount which depends on the latitude.

$$x_6 = x_5 + (\ell_e \, R \cos \phi' \, t_\ell) \, y_1 \qquad \text{and} \qquad y_6 = y_5 \tag{21}$$

where ω_e is the angular rate of the earth (about 72.722 micro-radians/sec) while ϕ' as before is the (geocentric) latitude, and R the distance of the surface from the center of the earth.

To obtain coordinates in the original system (x_e,y_e), we must add the coordinates of the sub-satellite point (x_o,y_o),

$$x_e = x_6 + x_o \qquad \text{and} \qquad y_e = y_6 + y_o \tag{22}$$

8. The Overall Transformation.

All the partial transformations can now be combined,

$$x_e = x_4 \cos H_s + y_4 \sin H_s + (\omega_e R t_\ell) \cos \phi' \, y_1 + x_o$$

$$y_e = -x_4 \sin H_s + y_4 \cos H_s + y_o$$

Or,

$$x_e = x_3 \cos H_s + y_3 \sin H_s + (\omega_e R t_\ell) \cos \phi' \, y_1 - (\alpha \cos H_s + \beta \sin H_s) z_o + x_o$$

$$y_e = -x_3 \sin H_s + y_3 \cos H_s - (-\alpha \sin H_s + \beta \cos H_s) z_o + y_o$$

That is,

$$x_e = \cos (H_s + \gamma) x_2 + \sin H_s \, y_2 + (\omega_e R t_\ell) \cos \phi' \, y_1 + x_o - (\alpha \cos H_s + \beta \sin H_s) z_o$$

$$y_e = -\sin (H_s + \gamma) x_2 + \cos H_s \, Y_2 + y_o - (-\alpha \sin H_s + \beta \cos H_s) z_o$$

Or,

$$x_e = \cos (H_s + \gamma)(\omega_m z_o t_s) x_1 + [\sin H_s (\omega_s R t_\ell) + \cos \phi' (\omega_e R t_\ell)] y_1 + [x_o - (\alpha \cos H_s + \beta \sin H_s) z_o]$$

$$y_e = -\sin (H_s + \gamma)(\omega_m z_o t_s) x_1 + \cos H_s (\omega_s R t_\ell) y_1 +$$

$$[y_o - (-\alpha \sin H_s + \beta \cos H_s) z_o]$$

9. Form of the Transformation.

The transformation is of the form,

$$x_e = a\ x_1 + b\ y_1 + c \tag{23}$$

$$y_e = d\ x_1 + e\ y_1 + f \tag{24}$$

This is an affine transformation, where the six parameters are given by

$$a = (\omega_m\ z_o\ t_s)\ \cos\ (H_s + \gamma) \tag{25}$$

$$b = (\omega_s\ R\ t_\ell)\ \sin\ H_s + (\omega_e\ R\ t_\ell)\ \cos\ \phi' \tag{26}$$

$$c = x_o - (\alpha\ \cos\ H_s + \beta\ \sin\ H_s)\ z_o \tag{27}$$

$$d = -(\omega_m\ z_o\ t_s)\ \sin\ (H_s + \gamma) \tag{28}$$

$$e = (\omega_s\ R\ t_\ell)\ \cos\ H_s \tag{29}$$

$$f = y_o - (-\alpha\ \sin\ H_s + \beta\ \cos\ H_s)\ z_o \tag{30}$$

We can use these equations to predict approximate transformation parameters from estimated values of satellite position, attitude and velocity in orbit. Conversely, if we can use ground control points or digital terrain models to determine the coefficients of the transformation more precisely, we can try and improve the estimates we have of satellite position and attitude.

From the form of the equations for c and f it becomes immediately clear, however, that there are some limits to this process. That is, one cannot dis-

tinguish in our model between displacements of the satellite across the track and small roll errors. Similarly, displacements along the track have the same effects as small pitch errors. Thus two of the six components of position and attitude cannot be found this way.

10. Attitude Rates.

Pitch, roll and yaw drift during the scanning of a single image. The rates are less than .015 degrees/second. A constant rate of change, $\dot{\beta}$ of pitch has the same effect as a change in along-track ground velocity of $\dot{\beta}\ z_o$. That is, equation (16) becomes,

$$y_2 = (\omega_s\ R + \dot{\beta}\ z_o)\ t_\ell\ y_1 \tag{31}$$

The transformation is altered only in the appearance of $(\omega_s\ R + \dot{\beta}\ z_o)\ t_\ell$ in place of $(\omega_s\ R\ t_\ell)$. Typical values for $\omega_s R$ and $\dot{\beta} z_o$ are 6458 and 32 meters/second respectively (when $\dot{\beta}$ = .002 degrees/second). This, then, is a small but noticeable change ($\approx$ .5%).

A constant rate of change, $\dot{\alpha}$, of roll has little effect on the scanning of a single line since $\omega_m\ z_o >> \dot{\alpha}\ z_o$. Successive lines, however, are shifted laterally by $\dot{\alpha}\ z_o\ t_\ell$. That is, equation (17) becomes,

$$x_3 = x_2 \cos\gamma + (\alpha\ z_o\ t_\ell)y_1 \quad \text{and} \quad y_3 = y_2 - x_2 \sin\gamma \tag{32}$$

This causes additional skewing of the image.

Here, typical values are $\omega_m\ z_o\ t_s \approx 56.5$ meters and $\dot{\alpha}\ t_o\ t_\ell \approx .4$ meter (for $\dot{\alpha}$ = .002 degree/second). Again we see a small, but noticeable change ($\approx$ .7%), resulting in additional skewing ($\approx$ .4%).

Finally, the transform parameters are now:

$$a = (\omega_m z_o t_s) \cos (H_s + \gamma) \tag{33}$$

$$b = (\omega_s R + \dot{\beta} z_o) t_\ell \sin H_s + (\dot{\alpha} z_o t_\ell) \cos H_s + (\omega_e R t_\ell) \cos \phi' \tag{34}$$

$$c = x_o - (\alpha \cos H_s + \beta \sin H_s) z_o \tag{35}$$

$$d = -(\omega_m z_o t_s) \sin (H_s + \gamma) \tag{36}$$

$$e = (\omega_s R + \dot{\beta} z_o) t_\ell \cos H_s - (\dot{\alpha} z_o t_\ell) \sin H_s \tag{37}$$

$$f = y_o - (-\alpha \sin H_s + \beta \cos H_s) z_o \tag{38}$$

We see here that the transformation parameters depend on the timing (t_s, t_ℓ) of the scanning system, the mirror scan velocity (ω_m), the position of the satellite relative to the tangent plane coordinate system (x_o, y_o, z_o), the orbital velocity vector (as it affects ω_s and H_s), the attitude of the scanner (α, β, γ), the attitude rates $(\dot{\alpha}, \dot{\beta}, \dot{\gamma})$, and the latitude, ϕ'.

The vertical component of the velocity vector (altitude rate) and also the yaw rate do not contribute to linear changes in the imaging transformation. The first produces a change of lateral scale from one end of the image to the other, the second a tilt of image lines at one end of the image relative to those at the other end. Such small, non-linear effects are ignored. Except for these two, however, all twelve components of the state of the scanner platform influence the transformation parameters.

If yaw rate and altitude rate <u>are</u> included, one finds small terms in $x_1 y_1$ (and y_1^2). The transformation is then no longer an affine transformation.

For small regions, the effects of these terms can be ignored -- for images which are large fractions of a standard LANDSAT image, they can not. In the latter case, one has to include other non-linear terms we have ignored in any case and then the transformation can be expressed with sufficient accuracy by two second-order polynomials.

11. Figure of the Earth.

To calculate the displacement of points due to the rotation of the earth, and to relate the geocentric distance of the satellite to its altitude above the surface, one needs to be able to calculate the distance of a point on the earth's surface from the earth's center. To a first approximation, a meridonal cross-section through the earth is an ellipse (Figure 8) with semi-major axis, a = 6,378,165 meters at the equator; and semi-minor axis, b = 6,356,783 meters at the poles.

If we introduce a coordinate system with the x-axis along the semi-major axis and the y-axis along the semi-minor axis, then the geocentric latitude, ϕ' is defined by,

$$\tan \phi' = y/x \tag{39}$$

The more commonly used geographic latitude, ϕ, is the angle between a local normal to the surface and the equatorial plane. Thus,

$$-1/\tan \phi = \frac{dy}{dx} \tag{40}$$

Using the equation for the ellipse,

$$(x/a)^2 + (y/b)^2 = 1$$

one finds that,

$$\frac{dy}{dx} = -\left(\frac{b}{a}\right)^2 \frac{x}{y}$$

so that

$$\tan \phi' = (b/a)^2 \tan \phi \tag{41}$$

Further,

$$x = \left(\frac{ab}{\sqrt{b^2 + a^2 \tan^2 \phi'}}\right)$$

$$y = \left(\frac{ab}{\sqrt{b^2 + a^2 \tan^2 \phi'}}\right) \tan \phi'$$

The distance of a point from the center, then, is,

$$R = \sqrt{x^2 + y^2} = \frac{ab}{\sqrt{a^2 \sin^2 \phi' + b^2 \cos^2 \phi'}} \tag{42}$$

The height of a surface feature above mean sea-level must be added to this.

12. Orbital Velocity.

Since one scanning motion depends on the satellite's angular velocity in its orbit, it is useful to relate this to other quantities. Using Kepler's second law, one immediately sees that

$$r^2 \frac{d\theta}{dt} = \frac{h}{2} \tag{43}$$

where r is the radius vector (geocentric altitude of the satellite), while h is a constant. Now the area of an ellipse with semi-major axis, a, and semi-minor axis, b, is πab, so that

$$\frac{h}{2} = \frac{2\pi}{T} ab$$

where T is the complete period of the satellite. Using ω_s for the angular velocity of the satellite, one finds,

$$\omega_s = \frac{2\pi}{T} \frac{ab}{r^2} = h \frac{ab}{r^2} \tag{44}$$

where the average angular rate $h = 2\pi/T$. Further,

$$h^2 a^3 = \mu = GM \tag{45}$$

by Kepler's third law, where G is the gravitational constant and M is the mass of the earth, $\mu \simeq 396.08 \times 10^{12}$ radian^2 meter^3/second^2.

For orbits with small eccentricity, there is very little difference between a and b, so perigee, r_p, and apogee, r_a, are given instead, where

$$\left.\begin{aligned} r_p &= a\,(1 - e) \\ r_a &= a\,(1 + e) \end{aligned}\right\} \tag{46}$$

and

$$a^2\,(1 - e^2) = b^2$$

Thus,

$$\left.\begin{aligned} a &= (r_a + r_p)/2 \\ b &= \sqrt{r_a\, r_p} \end{aligned}\right\} \tag{47}$$

$$e = \frac{r_a - r_p}{r_a + r_p} \tag{48}$$

Note that perigee and apogee are frequently given as distances from the surface of the earth and the equatorial radius of the earth (6,378,165 m) has to be added to this in order to find r_p and r_a. For a more detailed analysis, see Lyndanne's modification of Brouwer's analysis of satellite orbits.

13. Map Distortion.

So far we have ignored the fact that the spherical surface of the earth cannot be represented on a planar map without distortion. Up to this point, coordinates have been referred to a hypothetical plane tangent to the earth's surface at a point in the region of interest. Typically, a digital terrain model will be derived from a map with a different projection and a transformation must be established between the two coordinate systems.

It can be shown that for typical map projections such as transverse Mercator and conformal oblique axis cylindrical there exists a small rotation H_m of map coordinates, where

$$\sin H_m \simeq \sin \phi_o \sin (\theta - \theta_o) \tag{49}$$

Here the projection is centered on a point at longitude θ_o and latitude ϕ_o and the point of interest is at longitude θ and latitude ϕ. Consequently, the map coordinates, (x_m, y_m), are related to the geographical coordinates on the tangent plane (x_g, y_g) by

$$\begin{vmatrix} x_m \\ y_m \end{vmatrix} = \frac{1}{s} \begin{vmatrix} \cos H_m & -\sin H_m \\ \sin H_m & \cos H_m \end{vmatrix} \begin{vmatrix} x_g \\ y_g \end{vmatrix} \tag{50}$$

where s is the scale of the given map. There will also be a small scale change which varies with $1/\cos (\theta - \theta_o)$ for transverse Mercator and with $1/\cos (\phi - \phi_o)$ for conformal oblique axis cylindrical projection. Typically, this effect is

so small that it may be ignored.

The affine transformation, (23) and (24) must be pre-multiplied by an augmented rotation matrix M to correctly relate satellite image coordinates to map coordinates.

$$M = \frac{1}{s} \begin{vmatrix} \cos H_m & -\sin H_m & 0 \\ \sin H_m & \cos H_m & 0 \\ 0 & 0 & 1 \end{vmatrix} \tag{51}$$

14. Example of Map Rotation.

The national map of Switzerland is based on a conformal oblique axis cylindrical projection with center at the city of Bern.

$\theta_o \approx 7°26'20"$ $\phi_o \approx 46°57'10"$

The region of interest covered by an available terrain model lies at

$\theta \approx 7°8'$ $\phi \approx 46°15'$

The map rotation then is -.225° (-.00393 radians). The transformation matrix becomes

$$\begin{vmatrix} 1.0 & +.00393 \\ -.00393 & 1.0 \end{vmatrix}$$

(The scale error is less than one part in 10,000 and can be ignored). For more details regarding suitable map transformations see Colvocoresses paper on the "Space Oblique Mercator" projection.

15. Numerical Example -- Estimating Transform Parameters.

LANDSAT image number 1078-09555, produced 1972/October/9 shows a region of Switzerland including a mountain range called "Dent de Morcles". The image annotation data suggest that at the nadir the geographic latitude was 45.9197° and the heading 193.11324°. Using equation (41), we see that the geocentric latitude of the nadir point is 45.7274° and so, using equation (8), it appears that the orbital inclination must have been $\varepsilon \approx 9.11°$.

The altitude is given as 915,724 meters near the region of interest, which lies at an average of 1700 meters above average sea level. So $z_o \approx 914$ km. The angular velocity of the satellite is slightly above its average rate,

$$\omega_s = \frac{2\pi}{24 \times 60 \times 60} \times \frac{251}{18} \times 1.00967 \text{ radians/second}$$

The region of interest lies at geographic latitude $\phi = 46.25°$ (and thus at geocentric latitude $\phi' = 46.06°$), while the scanner at that time is above geographic latitude $\phi = 46.40°$ (that is, geocentric latitude $\phi' = 46.21°$).

Further,

$$\omega_e = \frac{2}{24 \times 60 \times 60} \text{ radians/second}$$

$$\omega_m = 6.21 \text{ radians/second}$$

$$t_s = 91958 \text{ } \mu\text{second}$$

$$t_\ell = \frac{1}{13.62 \times 6} \text{ seconds}$$

The image annotation also gives,

α (roll) = -.20370°	β (pitch) = .06688°	γ (yaw) = .23387°
$\dot{\alpha}$ = -.00160°/second	$\dot{\beta}$ = -.00109°/second	$\dot{\gamma}$ =.00189°/second

The earth radius (equation 42) near the region of interest is 6,367,081 meters. Adding the average elevation above sea level, we get

$$R \approx 6{,}368{,}800 \text{ meters}$$

Using equation (1), one finds that $\rho = 43.021°$ and by equation (8), that $H_s = 13.226°$. Further, $(H_s + \gamma) = 13.460°$. Then also, $\omega_m z_o t_s = 56.521$ meters, $(\omega_s R + \dot{\beta} z_o)t_\ell = 79.582$ meters, $\dot{\alpha} z_o t_\ell = -.312$ meter, and $\omega_e R t_\ell = 5.667$ meters.

So, finally,

$a = 54.969$ $\quad b = 21.837$ $\quad c = x_o + 2919$

$d = -13.156$ $\quad e = 77.543$ $\quad f = y_o - 1782$

See Figure 9 for a graphical illustration of this transformation. It shows as a parallelogram the region of the surface scanned when an image with a number of lines equal to the number of pixels per line is gathered.

We can take the inverse of the 2 x 2 sub-matrix and obtain,

$$x_1 = .01704\ x_e - .00480\ y_e + x'_o$$

$$y_1 = .00289\ x_e + .01208\ y_e + y'_o$$

where,

$$\begin{bmatrix} x'_o \\ y'_o \end{bmatrix} = -\begin{bmatrix} a & b \\ d & e \end{bmatrix}^{-1} \begin{bmatrix} c \\ f \end{bmatrix}$$

See Figure 10 for a graphical illustration of this transformation. It shows as a parallelogram the appearance in the image of a square region on the ground aligned with the north-south and east-west axes. Finally, if we have a terrain model on a 100 x 100 meter grid, such that $x_e = 100 * i$ and $y_e = 100 * j$, then,

$$x_1 = 1.704\ i - .480\ j + x'_o$$

$$y_1 = .289\ i - 1.208\ j + y'_o$$

Finally, we have to introduce the map distortion by <u>post-multiplying</u> by the <u>inverse</u> of the map transformation matrix introduced earlier (the inverse of a rotation matrix equals its transpose). The matrix then becomes

$$\begin{vmatrix} 1.702 & -.487 \\ .294 & 1.207 \end{vmatrix}$$

16. Determining Orbit Parameters from Transformation.

Many parameters appear in the equations for the six coefficients of the affine transformation. Some are known accurately, others only approximately. For example, t_s and t_ℓ are fixed fairly accurately by electronic oscillations on board the satellite. The angular rate of the earth ω_e is constant and accurately known, while ω_s, the angular rate of the satellite, depends on its altitude, semi-major axis, orbit eccentricity, and orbital period. The angular rate of the scanning mirror, ω_m, varies somewhat during each scan, though in a fairly repeatable fashion. The earth radius, R, can be calculated with sufficient accuracy if the latitude, ϕ', is known approximately.

It is reasonable, then, to assume that one can accurately predict a value for $\omega_e R t_\ell \cos \phi'$. Then let

$$b' = b - \omega_e R t_\ell \cos \phi'$$

The following equations permit the determination of useful satellite parameters from transformation parameters:

$$H_s + \gamma = \tan^{-1}(-d/a) \tag{52}$$

$$(\omega_m z_o t_s) = \sqrt{a^2 + d^2} \tag{53}$$

$$\sqrt{(\omega_s R + \dot{\beta} z_o)^2 + (\dot{\alpha} z_o)^2}\, t_\ell = \sqrt{(b')^2 + e^2} \tag{54}$$

If the heading H_s can be estimated, one finds

$$(\omega_s R + \dot{\beta} z_o)\, t_\ell = b' \sin H_s + e \cos H_s \tag{55}$$

$$(\dot{\alpha} z_o)\, t_\ell = b' \cos H_s \sin H_s \tag{56}$$

Alternatively, the heading can be calculated if the attitude rates are known,

$$H_s = \tan^{-1} \frac{b' (\omega_s R + \dot{\beta} z_o) - e (\dot{\alpha} Z_o)}{b' (\dot{\alpha} z_o) + e(\omega_s R + \dot{\beta} z_o)} \tag{57}$$

Clearly there are limitations to this, since the full state of the scanning platform cannot be ascertained from six parameters alone. A series of such measurements is needed to determine all twelve components of state.

17. Numerical Example.

Suppose the transformation matrix applicable to a 100 x 100 meter grid was found by image registration techniques using synthetic images,

$$\begin{bmatrix} 1.694 & -.512 \\ .300 & 1.216 \end{bmatrix}$$

for any area with a map distortion as defined previously. Post-multiplying by the map transformation matrix gives

$$\begin{bmatrix} 1.693 & -.505 \\ .295 & 1.217 \end{bmatrix}$$

The area is at geographical latitude $\phi = 46.25°$. The geocentric latitude is then $\phi' = 46.06°$ and so R = 6,367,081 meters. If the region of interest lies at an average altitude of 1700 meters, and $t_\ell = 1/(6 \times 13.62)$ seconds, then

$$\omega_e R t_\ell \cos \phi' = 3.932 \text{ meters/scan-line}$$

The inverse transformation matrix then is

$$\begin{bmatrix} 55.08 & 22.86 \\ -13.35 & 76.63 \end{bmatrix}$$

From this one finds,

$$H_s + \gamma = 13.624°$$

$$\omega_m z_o t_s = 56.67 \text{ meters/pixel}$$

And, if the attitude rates are assumed to be very small,

$$H_s = 13.874°$$

and so,

$$\gamma \simeq .251°$$

and

$$(\omega_s Rt_\ell) = 78.93 \text{ meters/scan-line.}$$

18. Using Ground Control Points.

An alternate method of estimating transformation parameters is based on the identification of points of known ground position in the image. Since the affine transformation has six parameters, one needs to locate three such points. Let the coordinates of the points be (x_1, y_1), (x_2, y_2) and (x_3, y_3) in the image and (x_1', y_1'), (x_2', y_2') and (x_3', y_3') on the map, then

$$x_i' = a\, x_i + b\, y_i + c$$

$$y_i' = d\, x_i + e\, y_i + f$$

and so on. Thus,

$$\begin{vmatrix} x_1 & y_1 & 1 \\ x_2 & y_2 & 1 \\ x_3 & y_3 & 1 \end{vmatrix} \begin{vmatrix} a \\ b \\ c \end{vmatrix} = \begin{vmatrix} x_1' \\ x_2' \\ x_3' \end{vmatrix}$$

So

$$\begin{vmatrix} a \\ b \\ c \end{vmatrix} = \begin{vmatrix} x_1 & y_1 & 1 \\ x_2 & y_2 & 1 \\ x_3 & y_3 & 1 \end{vmatrix}^{-1} \begin{vmatrix} x_1' \\ x_2' \\ x_3' \end{vmatrix}$$

Similarly,

$$\begin{vmatrix} f \\ e \\ f \end{vmatrix} = \begin{vmatrix} x_1 & y_1 & 1 \\ x_2 & y_2 & 1 \\ x_2 & y_3 & 1 \end{vmatrix}^{-1} \begin{vmatrix} y_1' \\ y_2' \\ y_3' \end{vmatrix}$$

If more than three points can be identified, better accuracy is available using a least-squares procedure. That is, if

$$M = \begin{vmatrix} x_1 & y_1 & 1 \\ x_2 & y_2 & 1 \\ & \vdots & \\ x_n & y_n & 1 \end{vmatrix}$$

Then a good set of values for the parameters is

$$\begin{vmatrix} a \\ b \\ c \end{vmatrix} = (M^T M)^{-1} M^T \begin{vmatrix} x_1' \\ x_2' \\ \vdots \\ x_n' \end{vmatrix}$$

$$\begin{vmatrix} d \\ e \\ f \end{vmatrix} = (M^T M)^{-1} M^T \begin{vmatrix} y_1' \\ y_2' \\ \vdots \\ y_n' \end{vmatrix}$$

Typically, the accuracy obtained by fitting a discrete set of ground control points has been found to be inferior to the area-based matching of real and synthetic images.

19. References.

1. Kratky, V., "Cartographic accuracy of ERTS", Photogrammetric Engineering, 40(2):203-212, 1974.

2. Steiner, D. and Kirby, M. E., "Geometrical referencing of LANDSAT images by affine transformation and overlaying of map data", Photogrammetria, 33:41-75, 1977.

3. Bernstein, R., "Digital image processing of earth observation sensor data", IBM Journal of Research and Development, 20(1):40-57, 1976.

4. LANDSAT Data Users Handbook, NASA 76SDS4258, Goddard Space Flight Center, Greenbelt, Maryland, 1976.

5. Bernstein, R., "All-digital precision processing of ERTS images", IBM Final Report to NASA, Contract NAS5-21716, Goddard Space Flight Center, Greenbelt, Maryland, 1975.

6. Rifman, S. S. and McKinnon, D. M., "Evaluation of digital correction techniques for ERTS images", TRW Corporation Final Report, TRW 20634060030TU-00, Contract NAS5-21814, Goddard Space Flight Center, Greenbelt, Maryland, 1974.

7. Thomas, Valerie, L., "Generation and physical characteristics of the LANDSAT 1 and 2 MSS Computer Compatible Tapes", NASA X-563-75-233, 1975.

8. Barnea, D. I. and Silverman, H. F., "The class of sequential similarity detection algorithms for fast digital image registration", IBM Research, RC3356, May, 1971.

9. Colvocoresses, A. P., "Space oblique mercator", Photogrammetric Engineering, :921-928, 1974.

10. Brouwer, D., "Solution of the problem of artificial satellite theory without drag", The Astronomical Journal, 64:378-397, November 1959.

11. Lynddane, R. H., "Small eccentricities or inclinations in the Brouwer theory of artificial satellite", The Astronomical Journal, 68:555-558, October 1963.

12. Horn, B. K. P. and Bachman, B. L., "Using synthetic images to register real images with surface models," M.I.T. Artificial Intelligence Laboratory Memo No. 437, August 1977.

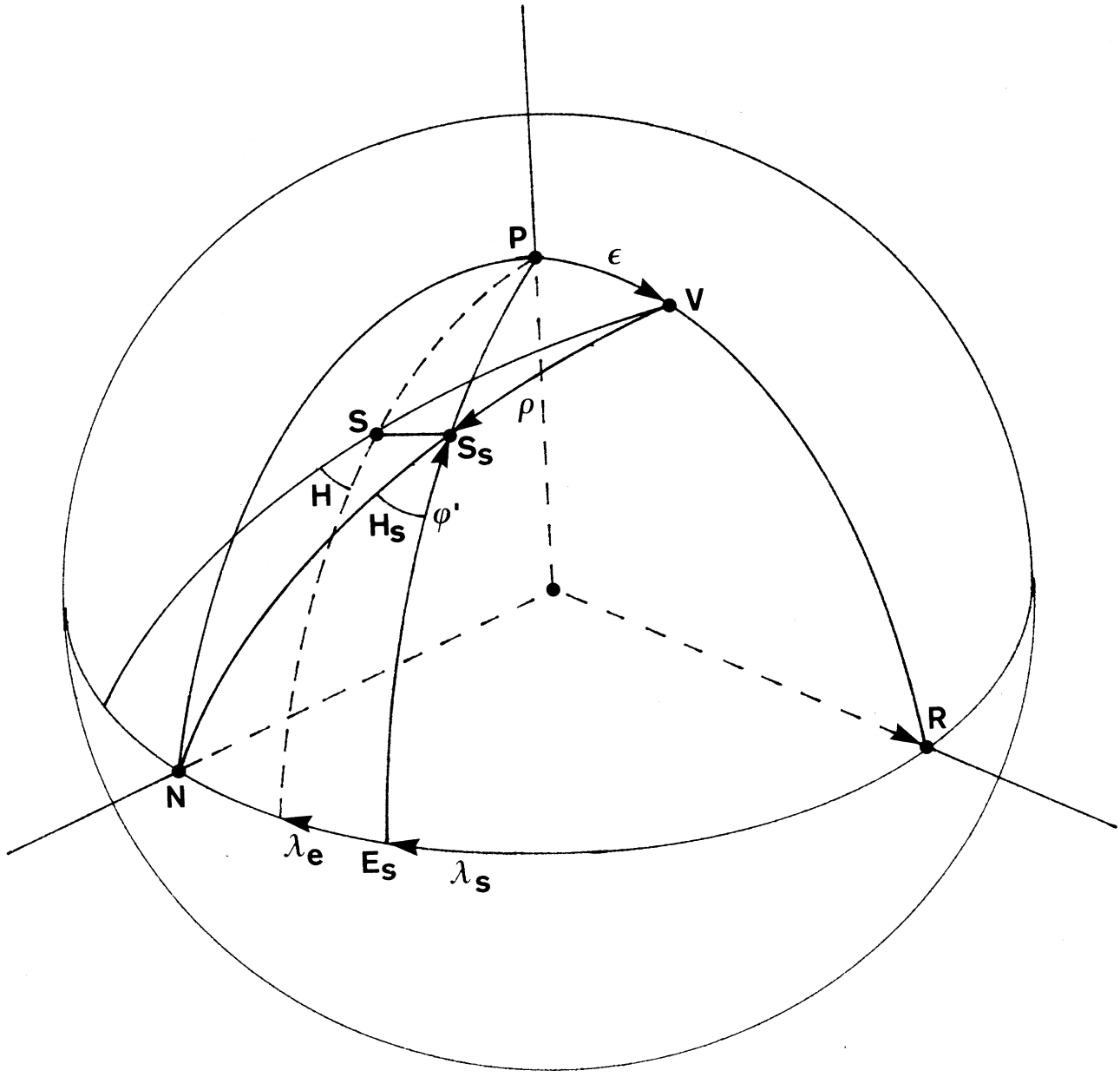

FIGURE I

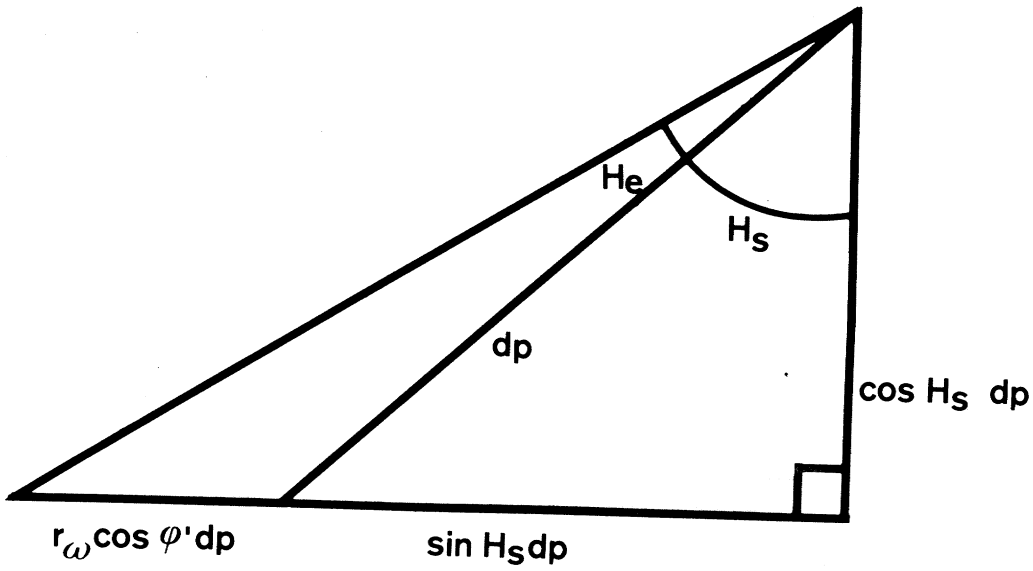

FIGURE 2

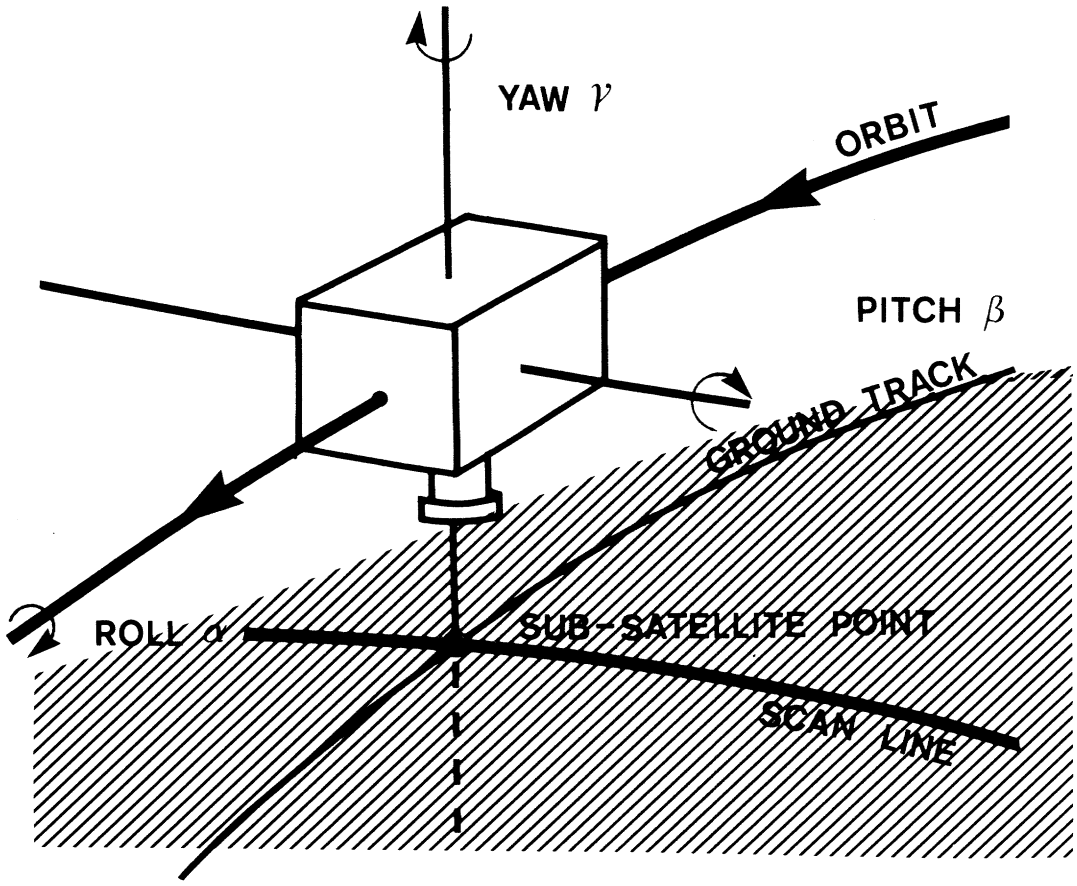
YAW γ
ORBIT
PITCH β
GROUND TRACK
ROLL α
SUB-SATELLITE POINT
SCAN LINE

FIGURE 3

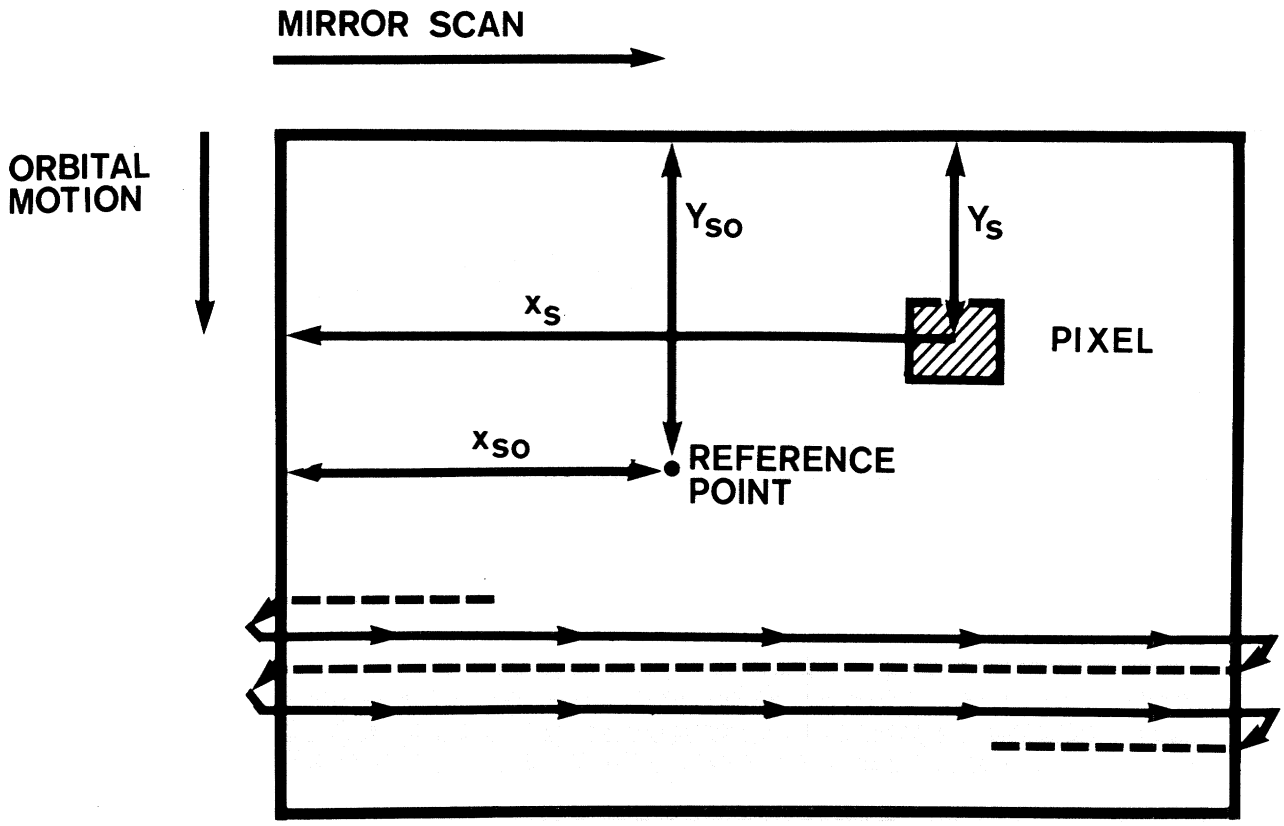
MIRROR SCAN
ORBITAL MOTION
Y_{so}
Y_s
x_s
PIXEL
x_{so}
REFERENCE POINT

FIGURE 4

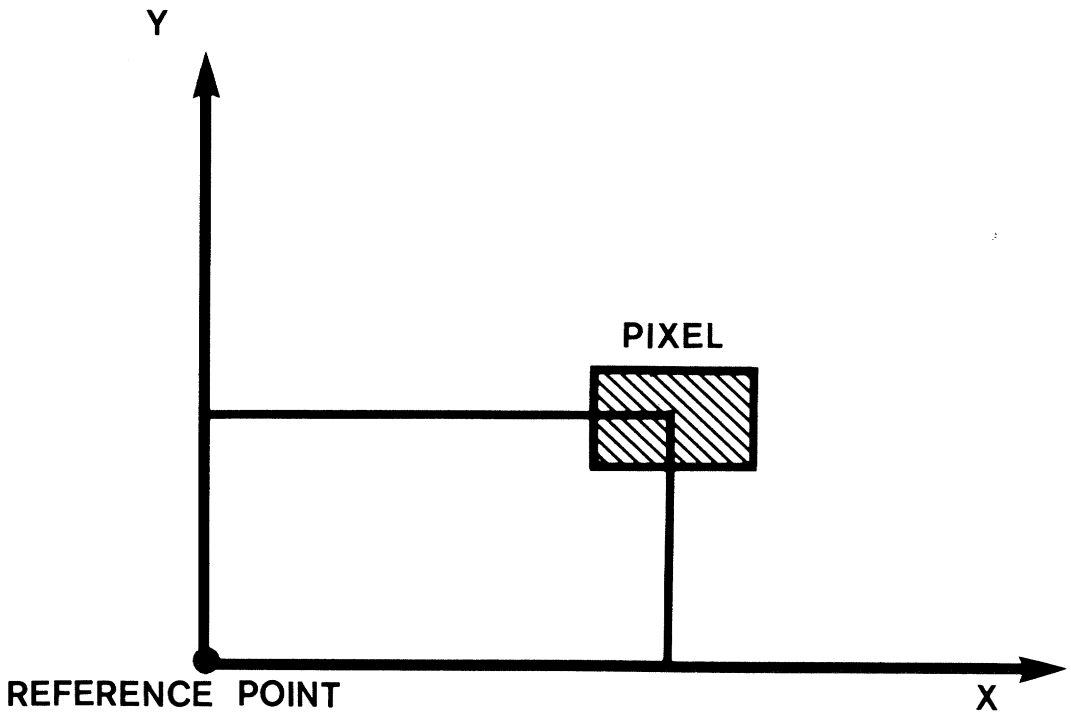

FIGURE 5

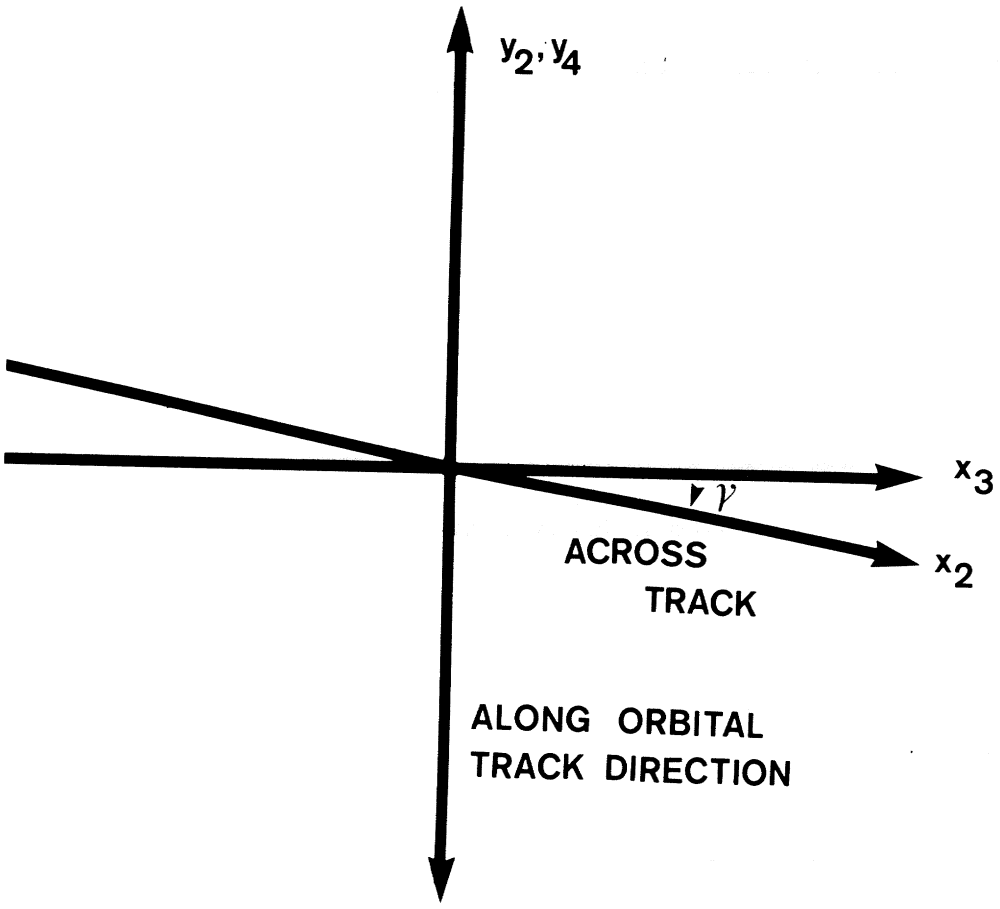
y_2, y_4
x_3
γ
x_2
ACROSS
TRACK
ALONG ORBITAL
TRACK DIRECTION

FIGURE 6

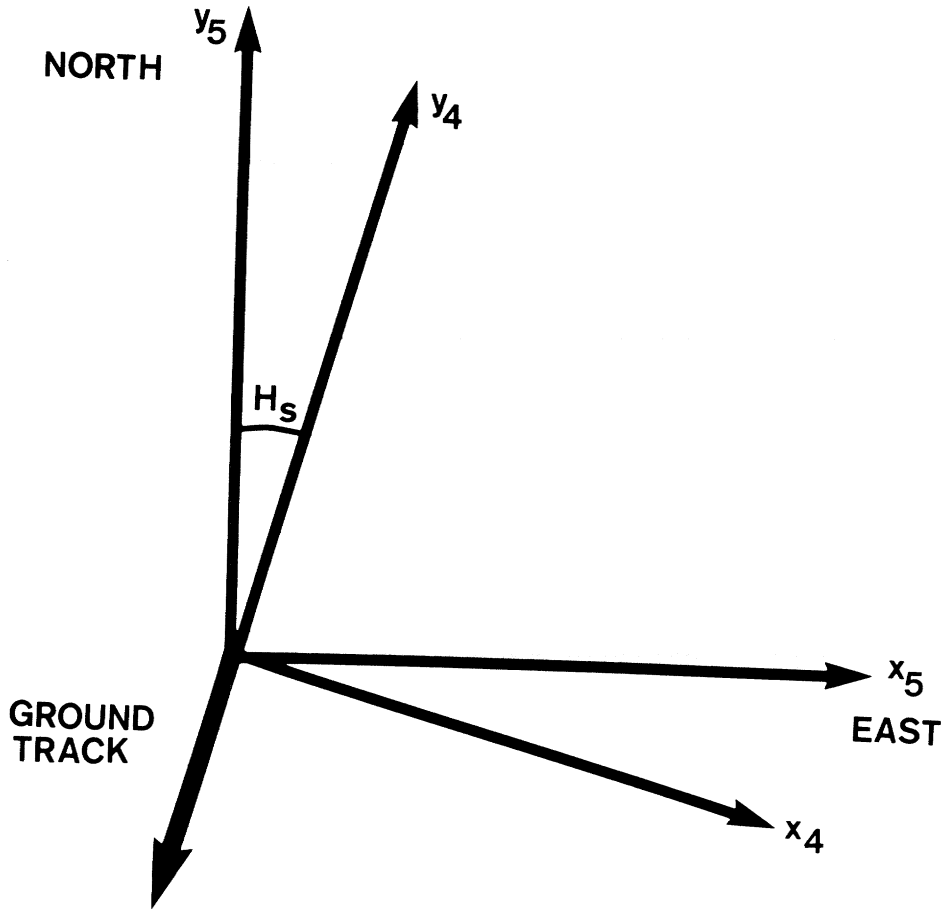

FIGURE 7

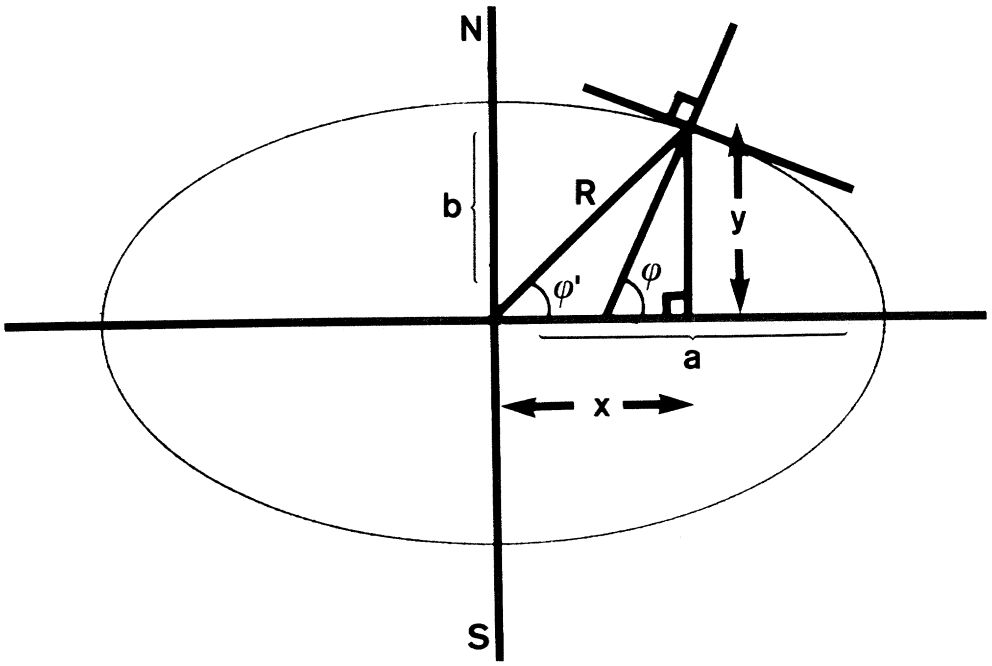

FIGURE 8

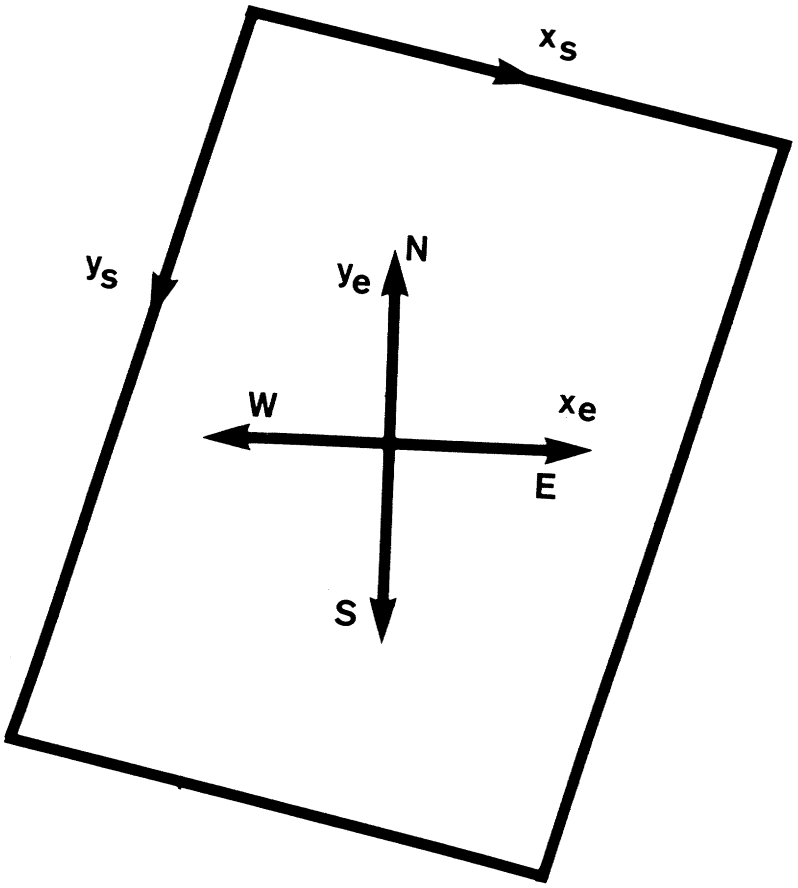

FIGURE 9

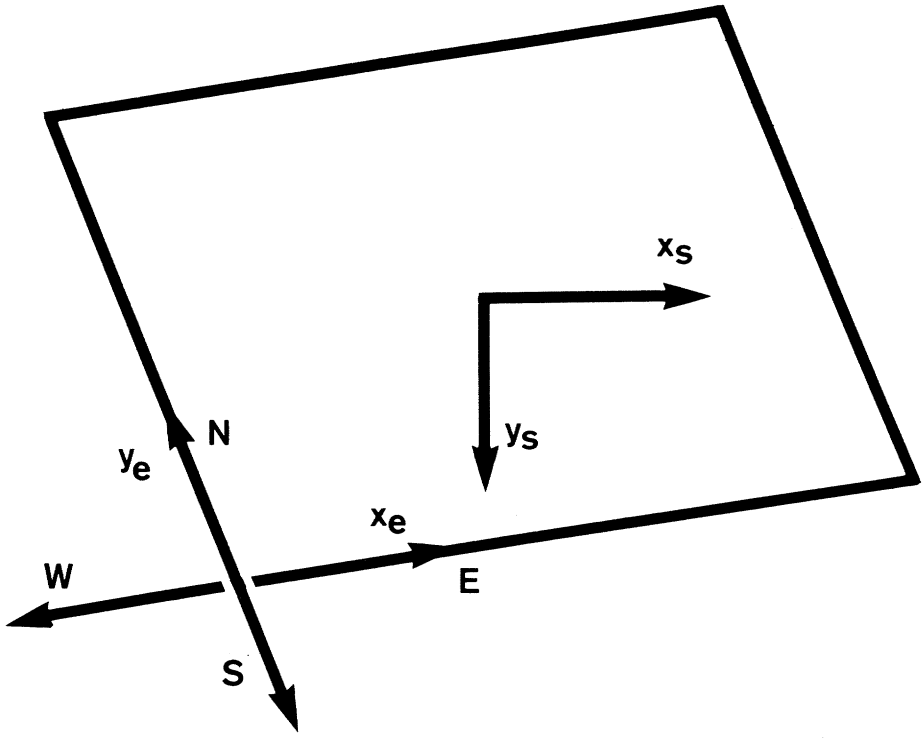

FIGURE IO